ADVANCED FUNCTIONAL MATERIALS

Supporting Information

for *Adv. Funct. Mater.*, DOI: 10.1002/adfm.201704561

Ultrafine Nickel-Nanoparticle-Enabled SiO_2 Hierarchical Hollow Spheres for High-Performance Lithium Storage

Chunjuan Tang, Yuning Liu, Chang Xu, Jiexin Zhu, Xiujuan Wei, Liang Zhou, Liang He, Wei Yang, and Liqiang Mai**

Supporting Information

Ultrafine Nickel Nanoparticle Enabled SiO_2 Hierarchical Hollow Spheres for High-Performance Lithium Storage

Chunjuan Tang, Yuning Liu, Chang Xu, Jiexin Zhu, Xiujuan Wei, Liang Zhou, Liang He, Wei Yang, Liqiang Mai**

Prof. C. J. Tang, Mr. Y. N. Liu, Ms. C. Xu, Mr. J. X. Zhu, Ms. X. J. Wei, Prof. L. Zhou, Prof. L. He, Mr. W. Yang, Prof. L. Q. Mai
State Key Laboratory of Advanced Technology for Materials Synthesis and Processing, International School of Materials Science and Engineering, Wuhan University of Technology, Wuhan 430070, P. R. China

Prof. L. Q. Mai
Department of Chemistry, University of California, Berkeley, California 94720, United States

Prof. C. J. Tang
Department of Mathematics and Physics, Luoyang Institute of Science and Technology, Luoyang, 471023, P. R. China

Keywords: hollow sphere, SiO_2, lithium storage, nanocomposite, synergistic effect

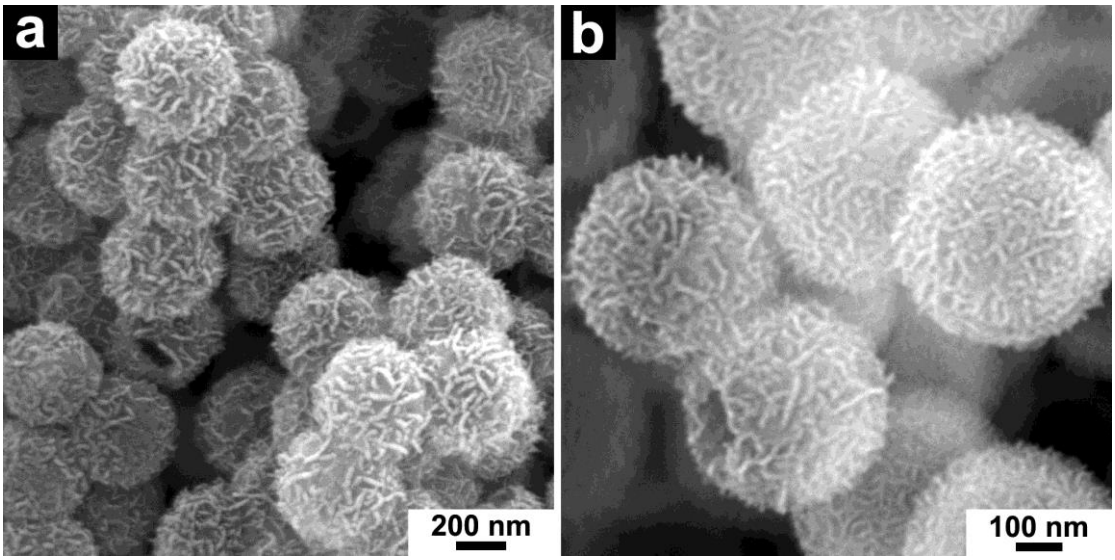

Figure S1. SEM images of nickel silicate hierarchical hollow spheres.

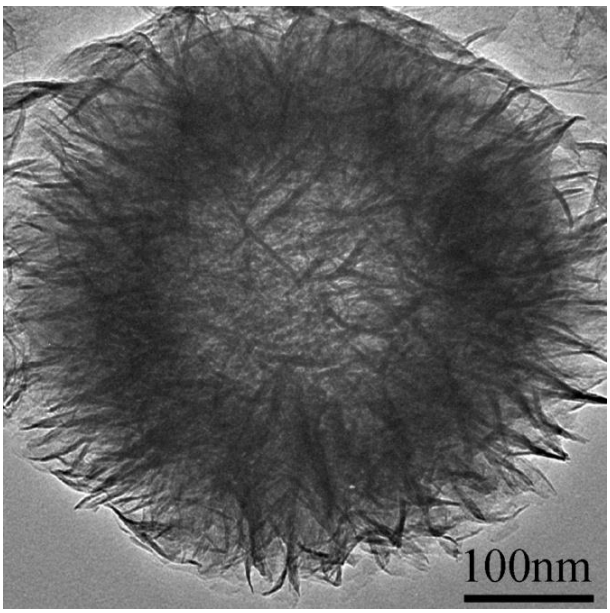

Figure S2. TEM image of nickel silicate hierarchical hollow spheres.

Table S1. ICP results of the Ni/SiO_2 nanocomposites.

	Ni/Si atomic ratio	**SiO_2 weight percentage (%)**
Ni/SiO_2-550	1.485:1	40.65
Ni/SiO_2-600	1.325:1	43.42
Ni/SiO_2-650	1.024:1	49.83
Ni/SiO_2-700	0.693:1	59.47

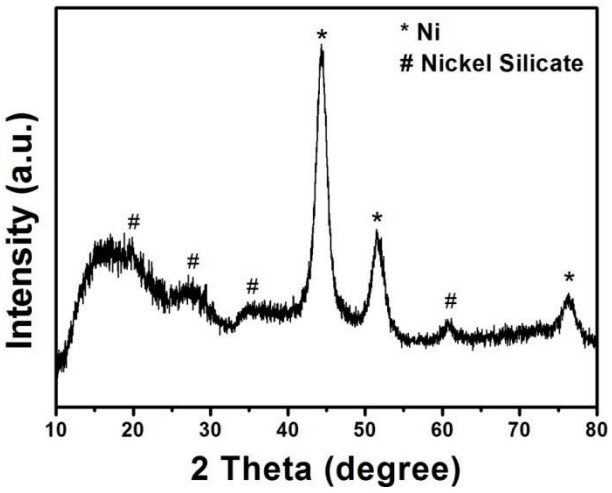

Figure S3. XRD pattern of the as-prepared product annealed at 500 ^{o}C for 16 h.

Table S2. BET surface areas of Ni/SiO_2 nanocomposites.

	Ni/SiO_2-550	**Ni/SiO_2-600**	**Ni/SiO_2-650**	**Ni/SiO_2-700**
BET Surface Area (m^2 g^{-1})	244	223	152	49

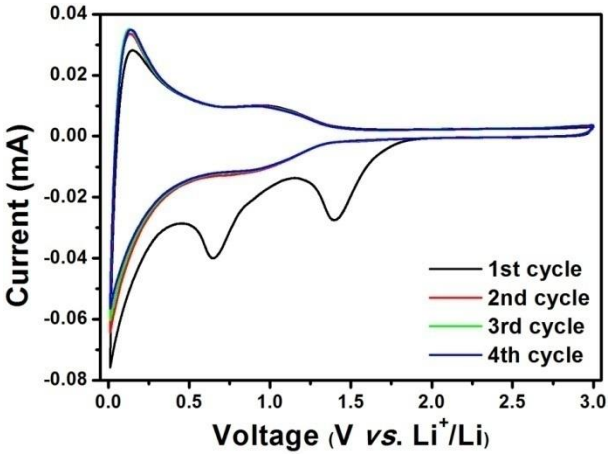

Figure S4. CV curves of the Ni/SiO_2-550 at a scan rate of 0.05 mV s^{-1}.

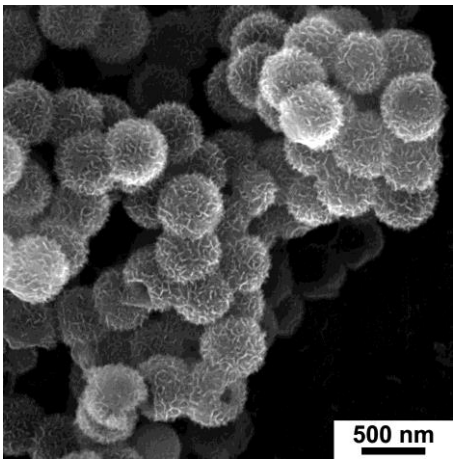

Figure S5. SEM image of pristine SiO_2 hierarchical hollow spheres.

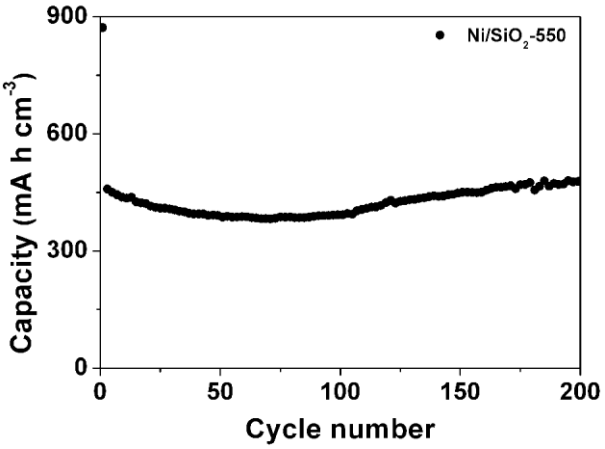

Figure S6. Volumetric capacity of Ni/SiO_2-550 versus cycle number. The volumetric capacity is calculated based on the weight of active material, thickness of the paste, and area of the electrode.

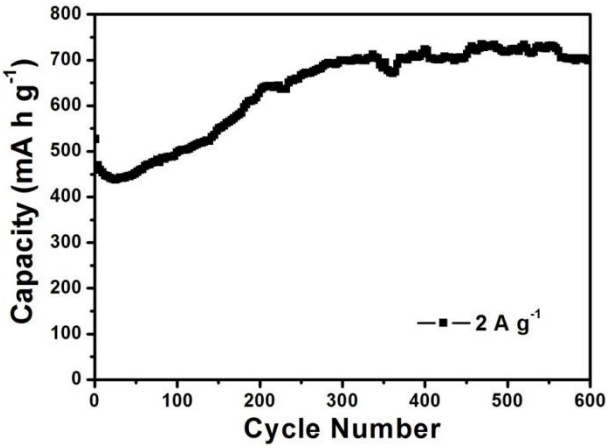

Figure S7. Cycling performance of Ni/SiO_2-550 at 2 A g^{-1}.

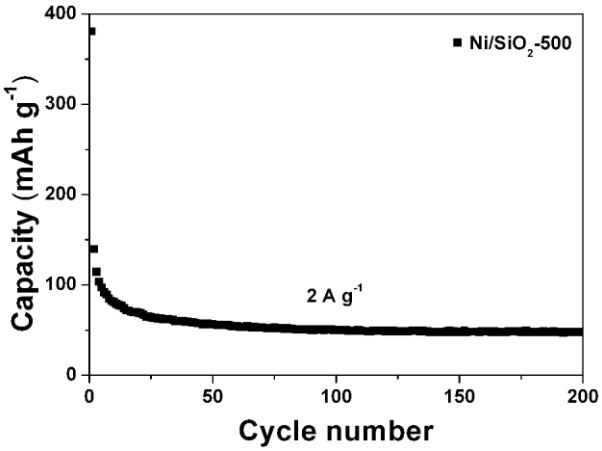

Figure S8. Cycling performance of Ni/SiO_2-500.

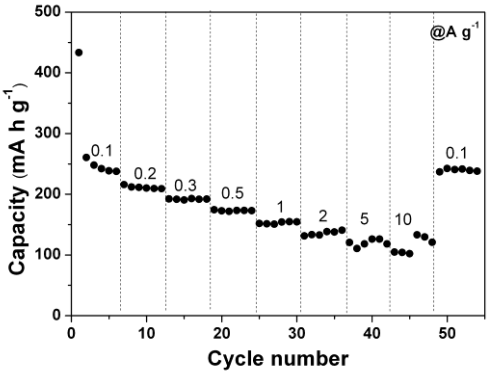

Figure S9. Rate performance of the pristine SiO_2.

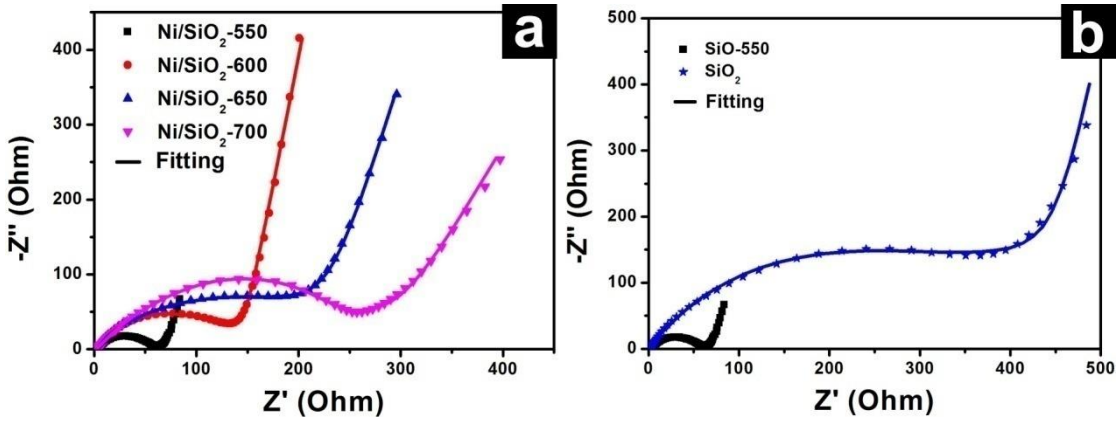

Figure S10. Nyquist plots of the Ni/SiO_2 nanocomposites (a) and Nyquist plots of pristine SiO_2 hierarchical hollow spheres and Ni/SiO_2-550 (b).

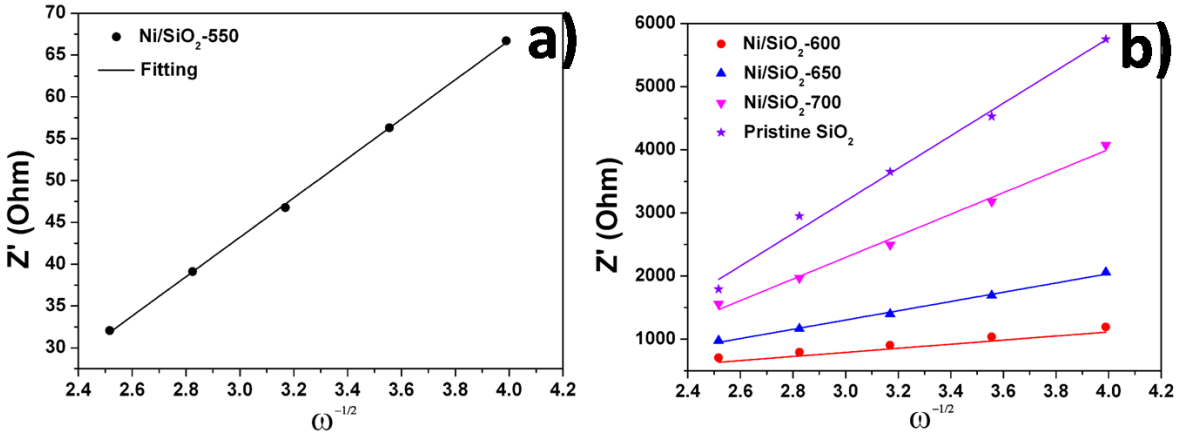

Figure S11. The relationship of Z' and $\omega^{-1/2}$ in the low frequency region of Ni/SiO_2-550 (a), Ni/SiO_2-600, Ni/SiO_2-650, Ni/SiO_2-700, and pristine SiO_2 (b).

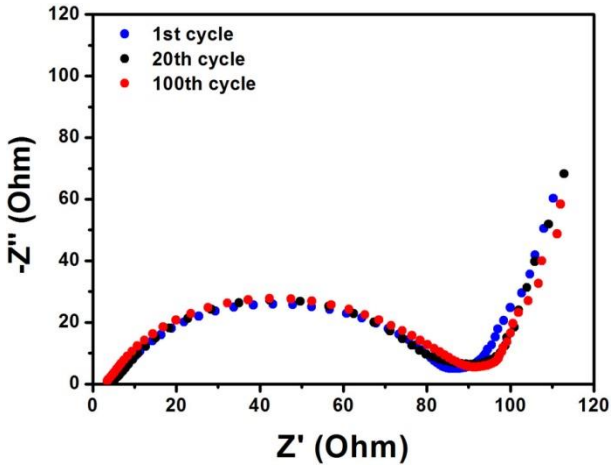

Figure S12. Nyquist plots of the Ni/SiO_2-550 composite electrode after the 1st, 20th, and 100th cycles.

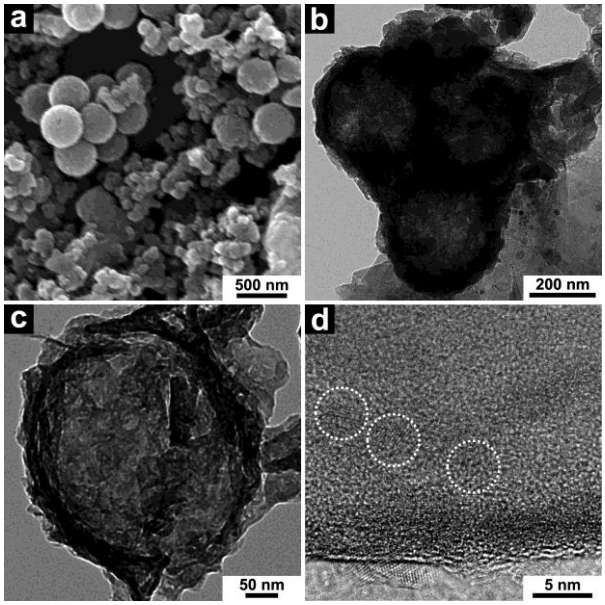

Figure S13. SEM (a), TEM (b, c), and HRTEM (d) images of Ni/SiO_2-550 after 100 discharge-charge cycles at 0.1 A g^{-1}.